Object Tracking in 3-D Space with Passive Acoustic Sensors using Particle Filter

Jinseok Lee[1], Shung Han Cho[2], Sangjin Hong[2], Jaechan Lim[3] and Seong-Jun Oh[4]
[1]Dept. of Biomedical Engineering,
Worcester Polytechnic Institute, Worcester, MA 01609 - USA
[e-mail : jinseok@wpi.edu]
[2]Mobile Systems Design Laboratory, Dept. of Electrical and Computer Engineering,
Stony Brook University-SUNY, Stony Brook, NY 11794 - USA
[e-mail: shcho, snjhong@ece.sunysb.edu]
[3]Dept. of Electronic Engineering, Sogang University,
Sinsu-Dong, Mapo-Gu, Seoul, 121-742 - South Korea
[e-mail: jaechan@gmail.com]
[4]College of Information and Communications, Korea University,
Anam-Dong, Seongbuk-Gu, Seoul, 136-713 - South Korea
[e-mail: seongjun@korea.ac.kr]
*Corresponding author: Seong-Jun Oh

Received May 26, 2011; revised August 4, 2011; accepted August 22, 2011;
published September 29, 2011

Abstract

This paper considers the object tracking problem in three dimensional (3-D) space when the azimuth and elevation of the object are available from the passive acoustic sensor. The particle filtering technique can be directly applied to estimate the 3-D object location, but we propose to decompose the 3-D particle filter into the three planes' particle filters, which are individually designed for the 2-D bearings-only tracking problems. 2-D bearing information is derived from the azimuth and elevation of the object to be used for the 2-D particle filter. Two estimates of three planes' particle filters are selected based on the characterization of the acoustic sensor operation in a noisy environment. The Cramer-Rao Lower Bound of the proposed 2-D particle filter-based algorithm is derived and compared against the algorithm that is based on the direct 3-D particle filter.

Keywords: Acoustic sensors, bearings-only tracking, 3-D object tracking, particle filter, data fusion

---

This research is supported in part by the International Collaborative R&D Program of the Ministry of Knowledge Economy (MKE), the Korean government, as a result of Development of Security Threat Control System with Multi-Sensor Integration and Image Analysis Project, 2010-TD-300802-002 and the the ITRC (Information Technology Research Center) support program supervised by the NIPA (National IT Industry Promotion Agency (NIPA-2011-(C1090-1121-0011)).

DOI: 10.3837/tiis.2011.09.008

1. Introduction

Locating and tracking an object using passive sensors both indoor and outdoor have been widely used in numerous applications. For tracking an object via passive sensors, several approaches based on the time-delay estimation (TDE) methods and beamforming methods have been proposed. The TDE method estimates location based on the time delay of the arrival of signals at the receivers [1]. The beamforming method uses the frequency-averaged output power of a steered beamformer [2][3]. The TDE method and beamforming method determine the current source location using the data obtained only at the current time. Each method transforms the acoustic data to a spatial data so that the peak represents the source location in a deterministic way.

The estimation accuracy of these methods, however, is sensitive to noise-corrupted signals. In order to overcome the drawback of these methods, a state-space driven approach based on particle filtering has been proposed [4][5]. The particle filtering is an emerging powerful tool for sequential signal processing, especially for nonlinear and non-Gaussian problems [6][7][8][9]. Tracking with particle filters for source localization is formulated in [10], where the TDE and beamforming methods are revised for the new framework. In [10], sensors are positioned at specified locations with constant height to estimate an object's trajectory in two dimensional (2-D) space. The extension to 3-D space from the revised TDE and beamforming methods is difficult, and a large number of microphones are required to generate a new 2-D plane for the 3-D extension. In addition, mobility of the sensors cannot be supported due to their fixed positions. In order to overcome the mobility problem, Direction of Arrival (DOA) based bearings-only tracking has been widely used in many applications [11][12][13]. In [14], acoustic sensors with DOA are incorportated with visual sensors for better accurate estimation in 2-D plane.

In this paper, we analyze the tracking methods based on passive sensors only to achieve flexible and accurate 3-D tracking. Tracking in 3-D has been addressed by directly extending 2-D bearings-only tracking problem to 3-D problem [15][16]. Instead of directly extending traditional particle filtering algorithms for bearings-only tracking in 3-D space, we propose to decompose the 3-D particle filter into several simpler particle filters designed for 2-D bearings-only tracking problems. The decomposition and planes selection are based on the characterization of the acoustic sensor operation under noisy environment. We use the passive acoustic localizer model in [17], where the two angle components (azimuth angle θ and elevation angle ϕ) between a sensor and an object are detected by the localizer. We compare the proposed approach with the directly extended bearings-only tracking method using Cramer-Rao Lower Bound.

The rest of this paper is organized as follows. Section 2 discusses the background and motivation, where we describe the sensor model and its noise characteristics. The general problem formulation and the dynamic model are also described. In Section 3, we describe the proposed method. Specifically, the Projected Planes Selection (PPS) method and planes combining scheme are discussed. Section 4 derives the Cramer-Rao Lower Bound (CRLB), and the simulation results are presented with CRLB in section 5. Finally, our contribution is summarized in Section 6.

2. Background and Problem Description

2.1 Problem Formulation for 3-D space Estimation

Consider an object's state vector $\mathbf{X}_n$, with discrete time instant $n \in \{1, 2, \cdots\}$, evolving according to

$$\mathbf{X}_n = f_{n-1}(\mathbf{X}_{n-1}) + \mathbf{Q}_{n-1}, \tag{1}$$

where f_{n-1} is a nonlinear dynamic transition function on state vector $\mathbf{X}_{n-1}$ and $\mathbf{Q}_{n-1}$ is a noise process (not-necessarily Gaussian) sampled at time instant $n-1$. The measurements of the object state vector is expressed as

$$\mathbf{Z}_n = h_n(\mathbf{X}_n) + \mathbf{E}_n, \tag{2}$$

where h_n is a nonlinear and time-varying observation function of state vector $\mathbf{X}_n$ and $\mathbf{E}_n$ is the measurement error referred to as a measurement noise sequence which is an independent identically distributed (IID) noise process. Then, the prediction probability density function (pdf) is obtained as

$$p(\mathbf{X}_n \mid \mathbf{Z}_{1:n-1}) = \int p(\mathbf{X}_n \mid \mathbf{X}_{n-1})\, p(\mathbf{X}_{n-1} \mid \mathbf{Z}_{1:n-1})\, \mathrm{d}\mathbf{X}_{n-1}, \tag{3}$$

where $\mathbf{Z}_{1:n}$ represents the sequence of measurements up to time instant n, and $p(\mathbf{X}_n \mid \mathbf{X}_{n-1})$ is the state transition density with Markov process of order one related to $f_n(\cdot)$ and $\mathbf{Q}_{n-1}$ in (1) [19]. Note that $p(\mathbf{X}_{n-1} \mid \mathbf{Z}_{1:n-1})$ is recursively obtained from previous time instants.

From the Bayes' rule, the estimation at the next time instant can be done as follow. The posterior pdf is obtained using the prediction pdf as

$$p(\mathbf{X}_n \mid \mathbf{Z}_{1:n}) = \frac{p(\mathbf{Z}_n \mid \mathbf{X}_n)\, p(\mathbf{X}_n \mid \mathbf{Z}_{1:n-1})}{\int p(\mathbf{Z}_n \mid \mathbf{X}_n)\, p(\mathbf{X}_n \mid \mathbf{Z}_{1:n-1})\, \mathrm{d}\mathbf{X}_n}, \tag{4}$$

where $p(\mathbf{Z}_n \mid \mathbf{X}_n)$ is the likelihood or measurement density in (2) related to the measurement model $h_n(\cdot)$ and the noise process $\mathbf{E}_n$, and the denominator is the normalizing constant. Note that the measurement $\mathbf{Z}_n$ is used to modify the prior density in (3) to obtain the current posterior density in (4) [19].

In this paper, $\theta_{xy,n}$ and $\mathbf{Z}_n(xy)$ are interchangeably used as the projected angle measurement in the xy-plane. Similarly, $\theta_{yz,n}$, $\mathbf{Z}_n(yz)$, $\theta_{zx,n}$, $\mathbf{Z}_n(zx)$ are for yz-plane and zx-plane, respectively. The state vectors of an object in 3-D space ($\mathbf{X}_n$) and in 2-D planes, ($\mathbf{X}_n(xy)$, $\mathbf{X}_n(yz)$, $\mathbf{X}_n(zx)$) are defined as

$$\mathbf{X}_n = \begin{pmatrix} x_n \\ V_n^x \\ y_n \\ V_n^y \\ z_n \\ V_n^z \end{pmatrix}, \mathbf{X}_n(xy) = \begin{pmatrix} x_n(xy) \\ V_n^x(xy) \\ y_n(xy) \\ V_n^y(xy) \end{pmatrix}, \mathbf{X}_n(yz) = \begin{pmatrix} y_n(yz) \\ V_n^y(yz) \\ z_n(yz) \\ V_n^z(yz) \end{pmatrix}, \text{ and } \mathbf{X}_n(zx) = \begin{pmatrix} z_n(zx) \\ V_n^z(zx) \\ x_n(zx) \\ V_n^x(zx) \end{pmatrix}, \tag{5}$$

where $\{x_n, y_n, z_n\}$ and $\{V_n^x, V_n^y, V_n^z\}$ are the true source location and the velocity in 3-D Cartesian coordinates at time instant n. $\{x_n(xy), y_n(xy)\}$ and $\{V_n^x(xy), V_n^y(xy)\}$ are the projected true source location and velocity on the xy-plane at time instant n; the same notation is applied for the yz- and zx-planes. Note that $x_n(xy)$ and $x_n(zx)$ are estimated separately and x_n is the finally fused value based on $x_n(xy)$ and $x_n(zx)$; the rest of components are applied in the same way. The three posterior pdf involving prediction probability density functions are given as

$$p(\mathbf{X}_n(xy) \mid \mathbf{Z}_{1:n}(xy)) = \frac{p(\mathbf{Z}_n(xy) \mid \mathbf{X}_n(xy))\, p(\mathbf{X}_n(xy) \mid \mathbf{Z}_{1:n-1}(xy))}{\int p(\mathbf{Z}_n(xy) \mid \mathbf{X}_n(xy))\, p(\mathbf{X}_n(xy) \mid \mathbf{Z}_{1:n-1}(xy))\, \mathrm{d}\mathbf{X}_n(xy)}, \tag{6}$$

$$p(\mathbf{X}_n(yz) \mid \mathbf{Z}_{1:n}(yz)) = \frac{p(\mathbf{Z}_n(yz) \mid \mathbf{X}_n(yz))\, p(\mathbf{X}_n(yz) \mid \mathbf{Z}_{1:n-1}(yz))}{\int p(\mathbf{Z}_n(yz) \mid \mathbf{X}_n(yz))\, p(\mathbf{X}_n(yz) \mid \mathbf{Z}_{1:n-1}(yz))\, \mathrm{d}\mathbf{X}_n(yz)}, \tag{7}$$

$$p(\mathbf{X}_n(zx) \mid \mathbf{Z}_{1:n}(zx)) = \frac{p(\mathbf{Z}_n(zx) \mid \mathbf{X}_n(zx))\, p(\mathbf{X}_n(zx) \mid \mathbf{Z}_{1:n-1}(zx))}{\int p(\mathbf{Z}_n(zx) \mid \mathbf{X}_n(zx))\, p(\mathbf{X}_n(zx) \mid \mathbf{Z}_{1:n-1}(zx))\, \mathrm{d}\mathbf{X}_n(zx)}. \tag{8}$$

Three 2-D estimates from the posterior pdfs given by equations (6), (7) and (8) can be used to estimate a single object's 3-D state vector. However, equations (6), (7) and (8) are only for the conceptual purpose, and they generally cannot be computed analytically except in special cases such as the linear Gaussian state space model. Instead of using those equations, for a nonlinear system, the particle filter can approximate the posterior pdf using a cloud of particles, and a sequential importance sampling (SIS) can be applied to perform the nonlinear filtering [9]. The particle filtering is further derived to the sequential importance resampling (SIR) algorithm, which chooses the candidates of importance density and performs the resampling at every time instant [20]. In this paper, we use the SIR particle filter that has a generic particle filtering algorithm for object tracking.

2.2 Dynamic Model and Observation Likelihood Function

Several dynamic models have been proposed to estimate the time-varying location and velocity. For the bearings-only tracking, three types of models are presented [13]. In the 2-D xy-plane, the constant velocity (CV) model, the clockwise coordinated turn (CT) model, and the anti-clockwise coordinated turn (ACT) model are expressed by state transition matrices $\mathbf{F}_n^{(1)}$, $\mathbf{F}_n^{(2)}$ and $\mathbf{F}_n^{(3)}$, respectively as

$$\mathbf{F}_n^{(1)} = \begin{pmatrix} 1 & T_s & 0 & 0 \\ 0 & 1 & 0 & 0 \\ 0 & 0 & 1 & T_s \\ 0 & 0 & 0 & 1 \end{pmatrix} \text{ and } \mathbf{F}_n^{(d)} = \begin{pmatrix} 1 & \sin(\Re_n^{(d)} T_s)/\Re_n^{(d)} & 0 & -(1-\cos(\Re_n^{(d)} T_s))/\Re_n^{(d)} \\ 0 & (1-\cos(\Re_n^{(d)} T_s))/\Re_n^{(d)} & 1 & \sin(\Re_n^{(d)} T_s)/\Re_n^{(d)} \\ 0 & \cos(\Re_n^{(d)} T_s) & 0 & -\sin(\Re_n^{(d)} T_s) \\ 0 & \sin(\Re_n^{(d)} T_s) & 0 & \cos(\Re_n^{(d)} T_s) \end{pmatrix}, \tag{9}$$

where T_s is the sampling period, d = 2,3 and $\Re_n^{(d)}$ is the mode-conditioned turning rate expressed as follows;

$$\Re_n^{(2)} = \frac{\alpha}{\sqrt{\left(V_n^x\right)^2 + \left(V_n^y\right)^2}} \text{ and } \Re_n^{(3)} = \frac{-\alpha}{\sqrt{\left(V_n^x\right)^2 + \left(V_n^y\right)^2}}, \tag{10}$$

where α is a constant for the rotated angle degree. In addition, the Constant Acceleration (CA) model in xy-plane is expressed as follows;

$$\mathbf{F}_n^{(4)} = \begin{pmatrix} 1 & \left(A_x T_s^2 / 2V_{n-1}^x\right) + T_s & 0 & 0 \\ 0 & \left(A_x T_s / V_{n-1}^x + 1\right) & 0 & 0 \\ 0 & 0 & 1 & \left(A_y T_s^2 / 2V_{n-1}^y\right) + T_s \\ 0 & 0 & 0 & \left(A_y T_s / V_{n-1}^y\right) + 1 \end{pmatrix}, \tag{11}$$

where A_x and A_y denote accelerations in the xy-plane for x- and y-directions, respectively. For the yz- and zx-planes, V^x and V^y in (10), and A_x and A_y in (11) are replaced according to the object state directional components. Furthermore, the CA model becomes the CV model when the values of A_x and A_y are zero.

The SIR particle filter operates as follows [20]. After a dynamic model propagates the sets of M particles for $\mathbf{X}_{n-1}^{(1:M)}(xy)$, $\mathbf{X}_{n-1}^{(1:M)}(yz)$ and $\mathbf{X}_{n-1}^{(1:M)}(zx)$, new sets of particles $\mathbf{X}_n^{(1:M)}(xy)$, $\mathbf{X}_n^{(1:M)}(yz)$\$, and $\mathbf{X}_n^{(1:M)}(zx)$ are generated. Then, the observation likelihood functions

$$p\left(\mathbf{Z}_n(xy) \middle| \mathbf{X}_n^{(1:M)}(xy)\right),\ p\left(\mathbf{Z}_n(yz) \middle| \mathbf{X}_n^{(1:M)}(yz)\right), \text{ and } p\left(\mathbf{Z}_n(zx) \middle| \mathbf{X}_n^{(1:M)}(zx)\right) \tag{12}$$

calculate the weights of the generated particles and estimate $\mathbf{X}_n(xy)$, $\mathbf{X}_n(yz)$ and $\mathbf{X}_n(zx)$ respectively, through the resampling processes.

2.3 Noisy Measurement Characterization on Projected Planes

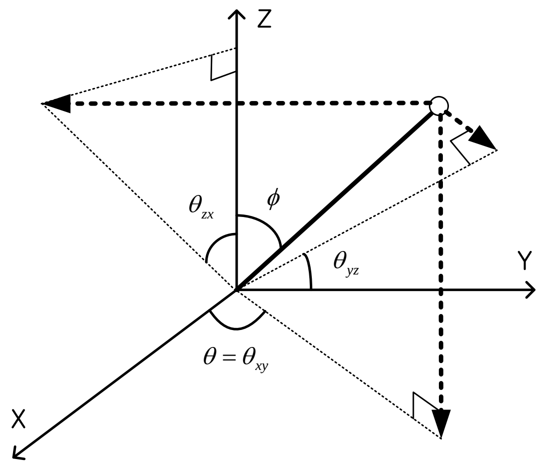

Fig. 1. Conversion of the original angles θ and ϕ to the projected angles θ_{xy}, θ_{yz} and θ_{zx}.

The 3-D localizer model and its implementation are described in [17], and it is based on the gradient flow to determine the DOA of the acoustic source. **Fig. 1** illustrates the simplified angle conversion process. Based on the two measured angles, azimuth θ and elevation ϕ, ($0 \le \theta < 2\pi$, $0 \le \phi < \pi$), three projected angles onto two dimensional (2-D) planes are derived; θ_{xy}, θ_{yz} and θ_{zx}. Each of these three angles can be used for 2-D tracking using the particle filter [18]. For example, θ_{xy} is used in xy-plane, θ_{yz} and θ_{zx} are used in yz-plane and zx-plane, respectively. The projected angles are derived and defined as

$$\theta_{xy} = \theta, \quad \theta_{yz} = \arctan\left(\frac{|\sec\theta|}{\tan\theta\tan\phi}\right) + \beta, \quad \theta_{zx} = \arctan\left(\frac{\tan\phi}{|\sec\theta|}\right) + \gamma, \tag{13}$$

where

$$\beta = \begin{cases} 0, & \text{for } y \ge 0, z \ge 0 \\ \pi, & \text{for } y < 0, \\ 2\pi, & \text{for } y \ge 0, z < 0, \end{cases} \quad \gamma = \begin{cases} 0, & \text{for } z \ge 0, x \ge 0 \\ \pi, & \text{for } x < 0, \\ 2\pi, & \text{for } z \ge 0, x < 0, \end{cases} \quad \text{and } \sec\theta = \frac{1}{\cos\theta} \tag{14}$$

We assume that each of the measurement errors of the original angles of θ and ϕ is and independent and identically distributed random sequence, respectively, and the two random sequences are independent. Also, we assume that the measurement errors are zero-mean with the same variance of σ^2. Then, the noisy measurements of θ and ϕ with the same error variance of σ^2 are reflected to the projected plane angles θ_{xy}, θ_{yz} and θ_{zx} with their own variances σ_{xy}^2, σ_{yz}^2, and σ_{zx}^2, respectively. Define the projected plane angles as

$$\theta_{xy,n} = \bar{\theta}_{xy,n} + e_n^{xy}, \quad \theta_{yz,n} = \bar{\theta}_{yz,n} + e_n^{yz}, \quad \theta_{zx,n} = \bar{\theta}_{zx,n} + e_n^{zx}, \tag{15}$$

where $\bar{\theta}_{\mathbb{P},n}$ is the projected true angle, $e_n^{\mathbb{P}}$ is the angle error with the variance $\sigma_{\mathbb{P}}^2$ in $\mathbb{P}$-plane at time instant n, and $\mathbb{P} \in \{xy, yz, zx\}$. Note that the original measurement error variance, σ^2, is differently projected to σ_{xy}^2, σ_{yz}^2 and σ_{zx}^2.

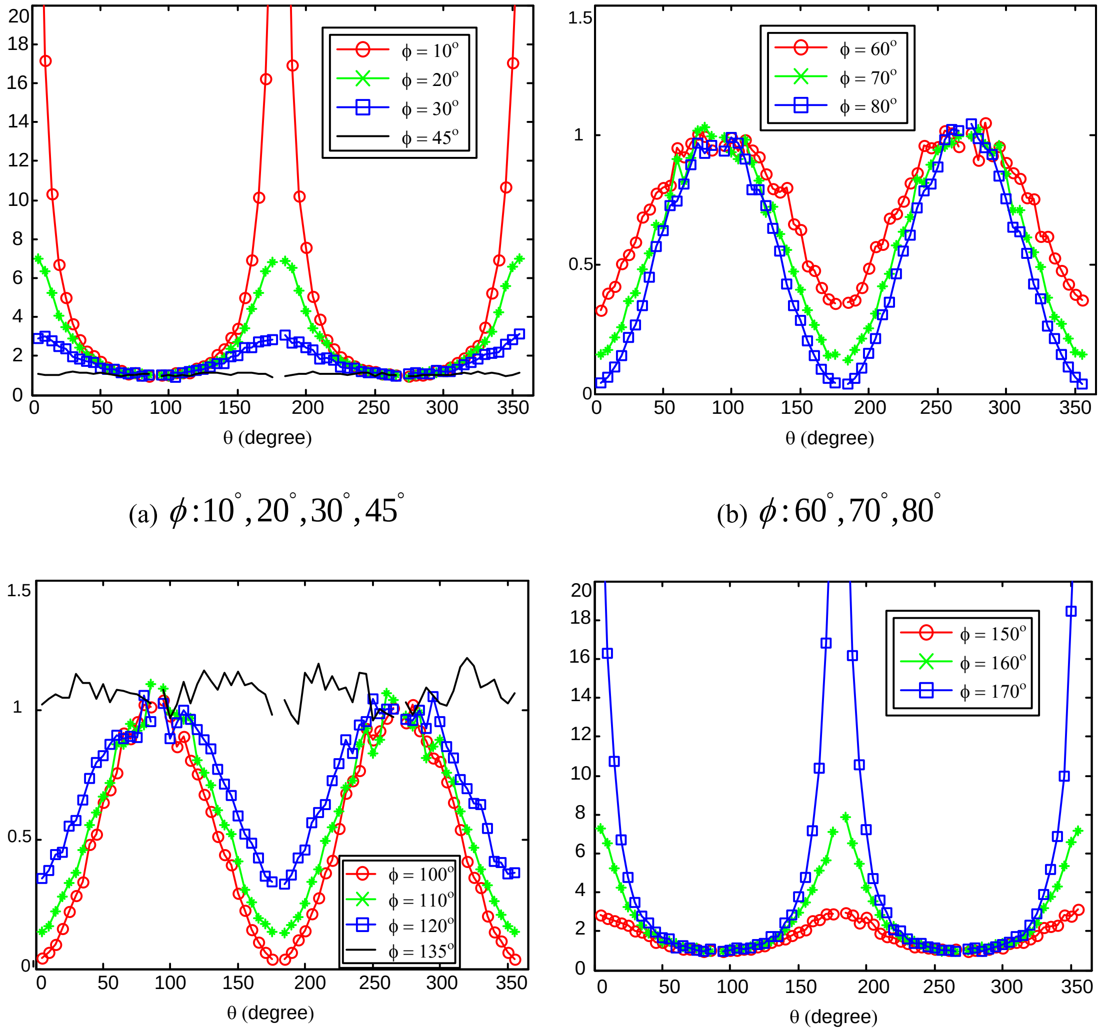

(a) $\phi: 10^\circ, 20^\circ, 30^\circ, 45^\circ$ (b) $\phi: 60^\circ, 70^\circ, 80^\circ$

(c) $\phi: 100^\circ, 110^\circ, 120^\circ, 135^\circ$ (d) $\phi: 150^\circ, 160^\circ, 170^\circ$

Fig. 2. Angle variances σ_{yz} in a projected yz-plane according to θ and ϕ. The originally measured

angle variances are 1. (x-axis: angle θ (degree), y-axis: variance)

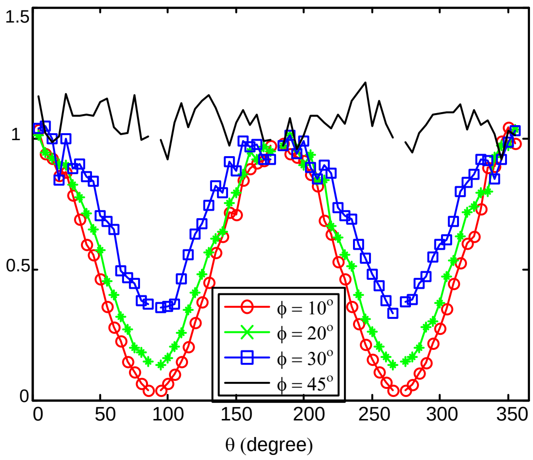

(a) ϕ:$10^{\circ}, 20^{\circ}, 30^{\circ}, 45^{\circ}$

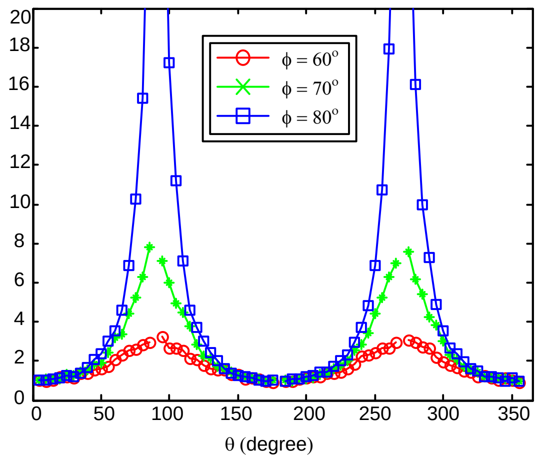

(b) ϕ:$60^{\circ}, 70^{\circ}, 80^{\circ}$

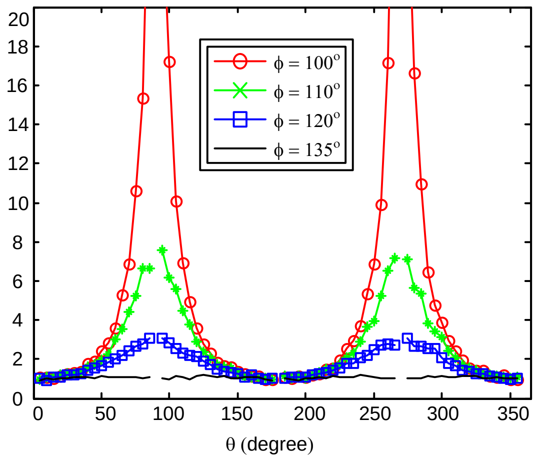

(c) ϕ:$100^{\circ}, 110^{\circ}, 120^{\circ}, 135^{\circ}$

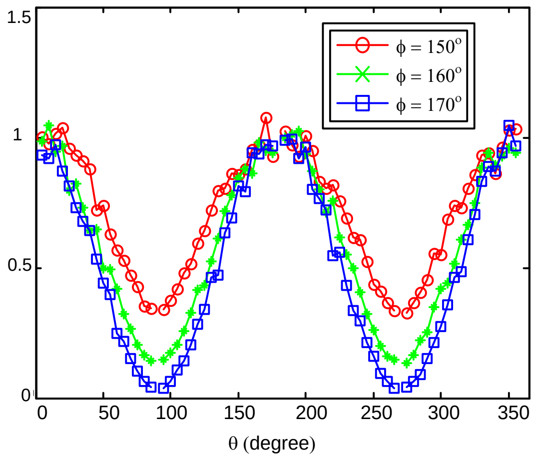

(d) ϕ:$150^{\circ}, 160^{\circ}, 170^{\circ}$

Fig. 3. Angle variances σ_{zx} in a projected zx-plane according to θ and ϕ. The originally measured angle variances are 1. (x-axis: angle θ (degree), y-axis: variance)

The projected angles from the original measurements θ and ϕ are derived in (13), but it is difficult to derive the closed-form expression for their variances from the variances of the original measurement errors – it requires the variance of products and variance of nonlinear functions. The results from the Monte-Carlo simulation in **Fig. 2** and **Fig. 3** show the projected angles' variances when the original measurements' variances are one. Note that the projected measurement in xy-plane, θ_{xy} is the same as the original θ; thus, σ_{xy}^2 is the same as σ^2. The projected variances in yz- and zx-planes are functions of θ and ϕ. In yz-plane, the elevation angles ϕ between 45° and 135° are projected with a smaller variance than the original measurement variance of one. In addition, as the azimuth angle θ approaches 0° or 180°, variance further decreases. For zx-plane, the other ranges of ϕ and θ are projected with a smaller variance than that of the original measurements.

3. Projected Planes Selection for Object Tracking in 3-D Space

3.1 Projected Planes Selection (PPS) Method

Planes Selection and Particles Generation: Instead of using the particle filter formulation with the direct 3-D state, the approach in this paper uses two of three possible 2-D particle filter formulations in order to estimate the 3-D state information. In the PPS method, we choose two planes with the smallest variance according to **Fig. 2** and **Fig. 3**. Note that xy-plane is always chosen because the projected variance in xy-plane is the second best plane with the same variance as the originally measured azimuth angle θ. The other yz- or zx-plane is selected based on the measured angle. For example, when ϕ is measured between 45^{o} and 135^{o}, the yz-plane is chosen. Otherwise, the zx-plane is chosen.

Once the two planes are selected, the two 2-D particle filters estimate the states separately. While the particle filters in the chosen planes estimate the state vectors, the particle filter in the other remained plane awaits for the selection. When the measured angles become close to the range where the projected measurement variance in the remained plane becomes less than the originally measured variance, the selected plane is switched.

There is always one redundant component that appears in both planes (i.e., y-component appears in xy-and yz-planes). As two particle filters are estimating the states separately, the redundant directional state from two particle filters may differ. For example, as discussed in (5), the intermediate 2-D object state vectors are given as $\left(x_n(xy), V_n^x(xy), y_n(xy), V_n^y(xy)\right)^T$ from the xy-plane particle filter and $\left(y_n(yz), V_n^y(yz), z_n(yz), V_n^z(yz)\right)^T$ from the yz-plane particle filter. Both $y_n(xy)$ and $y_n(yz)$ represent y directional position information, but the two values are different. Therefore, a combining method should be considered in order to get one final 3-D object state vector $\mathbf{X}_n$.

Redundancy Consideration in Combining Method: There are two ways to combine the two estimates of the state vectors of the y-direction's state vectors when xy- and yz- planes are selected; the planes weighted combining and the equal weight combining. In the planes weighted combining method, the two estimates are weighted according to the sum of weights of unnormalized particles in each plane's particle filter. This method is derived from the multiple particle filtering method [21], and extended to be combined into a final value with respect to the redundant state. Since a particle represents a point mass of the probability density, the sum of weights of unnormalized particles can be used in evaluating how the expected state is close to the true state [18][21][22]. The final 3-D object state vector $\mathbf{X}_n$ with the planes weighted combining method is obtained by

$$\mathbf{X}_n = \begin{pmatrix} 1 & 0 \\ 0 & 1 \\ 0 & 0 \\ 0 & 0 \\ 0 & 0 \\ 0 & 0 \end{pmatrix} \mathbf{X}_n(x \mid xyz) + \begin{pmatrix} 0 & 0 \\ 0 & 0 \\ 1 & 0 \\ 0 & 1 \\ 0 & 0 \\ 0 & 0 \end{pmatrix} \mathbf{X}_n(y \mid xyz) + \begin{pmatrix} 0 & 0 \\ 0 & 0 \\ 0 & 0 \\ 0 & 0 \\ 1 & 0 \\ 0 & 1 \end{pmatrix} \mathbf{X}_n(z \mid xyz), \tag{16}$$

where $\mathbf{X}_n(x \mid xyz)$, $\mathbf{X}_n(y \mid xyz)$ and $\mathbf{X}_n(z \mid xyz)$ are final 3-D estimated vectors with respect to each directional component representing $[x_n, V_n^x]^T$, $[y_n, V_n^y]^T$ and $[z_n, V_n^z]^T$, respectively. When the xy- and yz-planes are selected

$$\mathbf{X}_n(y \mid xyz) = \frac{\mathbf{X}_n(y \mid xy) \sum_{i=1}^{M} w_n^{(i)}(xy) + \mathbf{X}_n(y \mid yz) \sum_{i=1}^{M} w_n^{(i)}(yz)}{\sum_{i=1}^{M} w_n^{(i)}(xy) + \sum_{i=1}^{M} w_n^{(i)}(yz)}, \tag{17}$$

$$\mathbf{X}_n(x \mid xyz) = \mathbf{X}_n(x \mid xy), \text{ and } \mathbf{X}_n(z \mid xyz) = \mathbf{X}_n(z \mid yz), \tag{18}$$

where $\mathbf{X}_n(x \mid xy)$ and $\mathbf{X}_n(y \mid xy)$ represent the x and y directional 2-D state vectors in xy-plane, respectively. $\mathbf{X}_n(y \mid yz)$ and $\mathbf{X}_n(z \mid yz)$ represent the y and z directional 2-D state vectors in yz-plane. $w_n^{(i)}(xy)$ and $w_n^{(i)}(yz)$ are the i-th particle's weight of the particle filter for xy- and yz-plane at time instant n, and M represents the number of particles for each particle filter. Thus, the redundant y directional states are combined as in (17), where the weighting factors are $\sum_{i=1}^{M} w_n^{(i)}(xy)$ to xy-plane and $\sum_{i=1}^{M} w_n^{(i)}(yz)$ to yz-plane.

For the equal weight combining method, as it simply takes an average value, the redundant component y in (17) is replaced by

$$\mathbf{X}_n(y \mid xyz) = \frac{\mathbf{X}_n(y \mid xy) + \mathbf{X}_n(y \mid yz)}{2}. \tag{19}$$

3.2 Discussion

It has been assumed that the nonlinear dynamic transition function f_n is known as the state transition matrix $\mathbf{F}_n$ – as the particle filter is a model-based approach. If the dynamic model f_n changes in the middle of tracking, then the estimation from the particle filter can diverge. Divergence means that a predicted state and a true state continuously become more distant due to the unmatched model of a particle filter. Also, if the state of the unmatched model lasts longer, then the estimation may not recover even after recovering the model. The planes weighted combining method can discard the estimation from the plane with negligible sum of weights of unnormalized particles based on the likelihood function $p\left(\mathbf{Z}_n \middle| \mathbf{X}_n^{(1:M)}\right)$, and thus prevents estimation deviation. The equal weight combining and the planes weighted combining methods have similar tracking performance if all selected plane-particle filters show good tracking performances. However, when the tracking performance of one of the two particle filters deteriorates, the planes weighted combining method shows better performance.

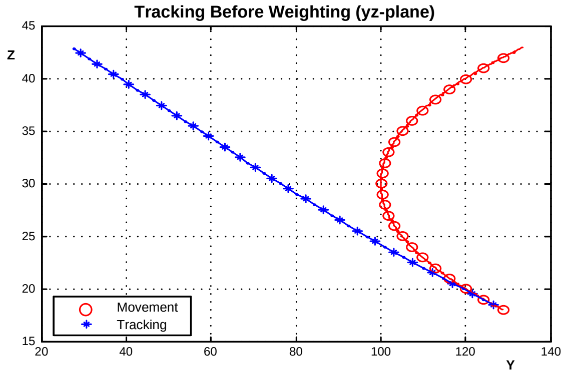

Fig. 4. Poor tracking in the yz-plane without combining methods. (Number of particles : 1,000).

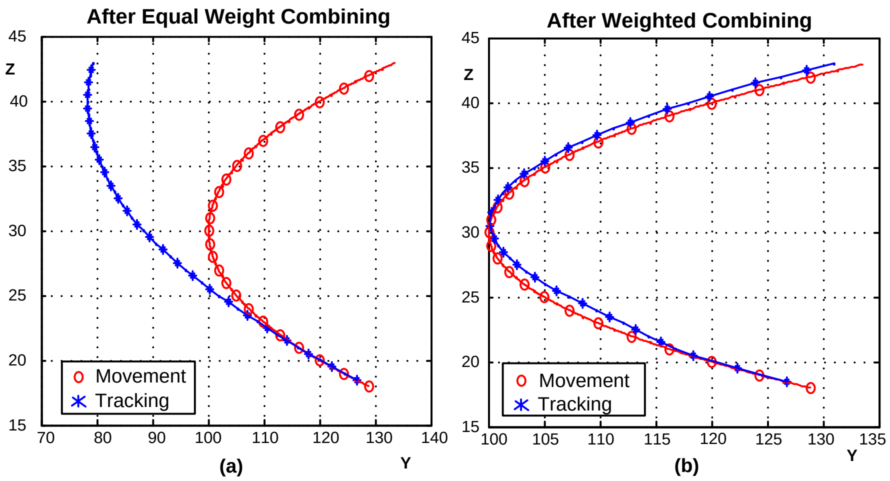

Fig. 5. Modified tracking performance with combining methods (Number of particles : 1,000) (a) Equal weight combining method (b) Weighted combining method.

Tracking performance is shown in **Fig. 4** and **Fig. 5**, where the particle filter in yz-plane results in a deviated estimation. Since the xy- and yz-planes are selected, the y direction's state estimates are combined. **Fig. 4** shows an example of tracking deviation in the yz-plane due to the unmatched model or a particle filter's performance degradation. **Fig. 5** shows a final estimation after applying two combining methods. Especially in **Fig. 5(b)**, it is shown that the planes weighted combining method maintains the object tracking by considering the contribution of the sum of weights of unnormalized particles from different planes. *PPS Versus Direct 2-D Method*: The 3-D object state model directly uses two original measurements and a cone shape likelihood function for assigning 3-D distributed particle weights **[23]**. The direct 3-D Method uses the two original measurements with σ^2, while the PPS method uses two projected measurements with σ_{xy}^2 and $\min(\sigma_{yz}^2, \sigma_{zx}^2)$. **Fig. 6** shows the sum of weights of unnormalized particles corresponding to the selected yz-plane and the direct 3-D model. It is shown that the selected plane is less sensitive to measurement noise than the direct 3-D model; thus, the unnormalized particles weight-sums of PPS method is larger than those of the direct 3-D Method. In addition, the direct 3-D Method cannot achieve redundancy, and thus there is no opportunity to avoid performance degradation when a particle filter has poor performance. The performances are compared according to the Cramer-Rao Lower bound (CRLB) in Section 4.

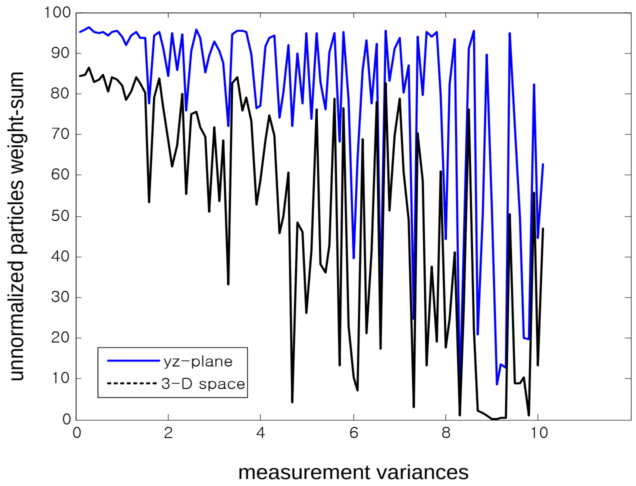

Fig. 6. Comparison between the selected yz - planes and 3-D space: unnormalized particles weight-sums according to the variances of original measurements (The number of particles: 100).

4. Cramer-Rao Lower Bound Derivation and Performance Analysis

The Cramer-Rao Lower Bound (CRLB) has been widely used as a reference in evaluating an estimator by representing the minimum covariance of the estimated states that an unbiased estimator can achieve. For the object tracking problem with bearings-only measurements, the CRLB is investigated in [24], and similar approaches are taken in this paper. As in [24], we assume that the process noise $\mathbf{Q}_n$ is zero and the dynamic models are fixed and known; otherwise, the derivation is intractable. The covariance matrix of the state estimate $\hat{\mathbf{X}}_n$ is given as follows

$$\mathbf{C}_n = E\left[\left(\hat{\mathbf{X}}_n - \mathbf{X}_n\right)\left(\hat{\mathbf{X}}_n - \mathbf{X}_n\right)^T\right] \geq \mathbf{J}_n^{-1} \tag{20}$$

where $\mathbf{J}_n$ is the information matrix, and it is defined as

$$\mathbf{J}_n = E\left\{\left[\nabla_{\mathbf{X}_n} \log p(\mathbf{X}_n \mid \mathbf{Z}_n)\right]\left[\nabla_{\mathbf{X}_n} \log p(\mathbf{X}_n \mid \mathbf{Z}_n)\right]^T\right\}, \tag{21}$$

where $\nabla_{\mathbf{X}_n}$ denotes the gradient operator with respect to the state vector $\mathbf{X}_n$, and $p(\mathbf{X}_n \,|\, \mathbf{Z}_n)$ is the conditional pdf of state $\mathbf{X}_n$ given the observation $\mathbf{Z}_n$. Note that the inequality of the square matrix in (20) means that matrix $\mathbf{C}_n - \mathbf{J}_n^{-1}$ is positive definite. The CRLB's of the components in the state vector $\mathbf{X}_n$ is the lower bound of its variance, and it is the diagonal elements of the inverse matrix of $\mathbf{J}_n$ [25].

We do not directly obtain the information matrix as in (21), but it is derived recursively as follows. In the absence of process noise, the evolution of state vector is deterministic, and it is given as [19][26]

$$\mathbf{J}_{n+1} = \left[\mathbf{F}_n^{-1}\right]^T \mathbf{J}_n \mathbf{F}_n^{-1} + \mathbf{H}_{n+1}^T \mathbf{R}_{n+1}^{-1} \mathbf{H}_{n+1}, \tag{22}$$

where $\mathbf{F}_n$ is the state transition matrix that represents CV or CA as shown in (10) and (11), respectively, $\mathbf{R}_{n+1}$ is the covariance matrix of the bearing measurements and $\mathbf{H}_n$ is the gradient component of a measurement function h_n. $\mathbf{H}_n$ is referred to as the Jacobian of h_n, and it is given as follows

$$\mathbf{H}_n = \left(\nabla_{\mathbf{X}_n} h_n^T(\mathbf{X}_n)\right)^T. \tag{23}$$

In the following subsections, the CRLB's of the PPS method are compared against the direct 3-D Method. The dynamic model of interest is assumed to be CV in the x-axis, CA with A_y and A_z in the y and z-axis.

4.1 CRLB Derivation based on the PPS Method

In the PPS method, two information matrices in (22) are generated for each selected plane. For clear notation, we put the plane type $\mathbb{P}$ as $\mathbf{J}_n^{\mathbb{P}}$, which represents $\mathbf{J}_n^{xy}$, $\mathbf{J}_n^{yz}$ or $\mathbf{J}_n^{zx}$. Similarly, the transition matrix, measurement variance and Jacobian of h_n are also denoted as $\mathbf{F}_n^{\mathbb{P}}$, $\mathbf{R}_n^{\mathbb{P}}$ and $\mathbf{H}_n^{\mathbb{P}}$, respectively for $\mathbb{P} \in \{xy, yz, zx\}$. From (9) and (11), transition matrices $\mathbf{F}_n^{\mathbb{P}}$'s are derived as

$$\mathbf{F}_n^{xy} = \begin{pmatrix} 1 & T_s & 0 & 0 \\ 0 & 1 & 0 & 0 \\ 0 & 0 & 1 & A_y T_s^2 / 2V_{n-1}^y + T_s \\ 0 & 0 & 0 & A_y T_s / V_{n-1}^y + 1 \end{pmatrix}, \quad \mathbf{F}_n^{zx} = \begin{pmatrix} 1 & A_z T_s^2 / 2V_{n-1}^z + T_s & 0 & 0 \\ 0 & A_z T_s / V_{n-1}^z + 1 & 0 & 0 \\ 0 & 0 & 1 & T_s \\ 0 & 0 & 0 & 1 \end{pmatrix}, \tag{24}$$

and

$$\mathbf{F}_n^{yz} = \begin{pmatrix} 1 & A_y T_s^2 / 2V_{n-1}^y + T_s & 0 & 0 \\ 0 & A_y T_s / V_{n-1}^y + 1 & 0 & 0 \\ 0 & 0 & 1 & A_z T_s^2 / 2V_{n-1}^z + T_s \\ 0 & 0 & 0 & A_z T_s / V_{n-1}^z + 1 \end{pmatrix}. \quad (25)$$

In the PPS method, the covariance matrix of measurement, $\mathbf{R}_n^{\mathrm{P}}$ becomes σ_{xy}^2, σ_{yz}^2 or σ_{zx}^2, which is the variance of a single (projected) bearing measurement in the projected plane xy, yx or zx-plane, respectively. The performance of the PPS method is mainly enhanced by taking only the measurement with smaller variance. According to **Fig. 2** and **Fig. 3**, the raw bearings, θ and ϕ, are projected onto the three planes with the different angle variances according to the object's position.

For Jacobians in the xy-plane, $\mathbf{H}_{n+1}^{xy}$ is derived from

$$h_{n+1}^T\left(\mathbf{X}_{n+1}(xy)\right) = \theta_{xy}\left(\mathbf{X}_{n+1}(xy)\right) = \arctan\left(\frac{y_{n+1}}{x_{n+1}}\right) \quad (26)$$

and

$$\frac{\partial}{\partial x_{n+1}} \arctan\left(\frac{y_{n+1}}{x_{n+1}}\right) = \frac{-y_{n+1}}{x_{n+1}^2 + y_{n+1}^2}, \quad \frac{\partial}{\partial y_{n+1}} \arctan\left(\frac{y_{n+1}}{x_{n+1}}\right) = \frac{x_{n+1}}{x_{n+1}^2 + y_{n+1}^2},$$

$$\frac{\partial}{\partial V_{n+1}^x} \arctan\left(\frac{y_{n+1}}{x_{n+1}}\right) = \frac{\partial}{\partial V_{n+1}^y} \arctan\left(\frac{y_{n+1}}{x_{n+1}}\right) = 0. \quad (27)$$

Then,

$$\mathbf{H}_{n+1}^{xy} = \left(\nabla_{\mathbf{X}_{n+1}(xy)} h_{n+1}^T(\mathbf{X}_{n+1}(xy))\right)^T = \left(\frac{-y_{n+1}}{x_{n+1}^2 + y_{n+1}^2},\ 0,\ \frac{x_{n+1}}{x_{n+1}^2 + y_{n+1}^2},\ 0 \right), \quad (28)$$

and by the same way, the Jacobians for yz- and zx-planes are derived as follows

$$\mathbf{H}_{n+1}^{yz} = \left(\frac{-z_{n+1}}{y_{n+1}^2 + z_{n+1}^2},\ 0,\ \frac{y_{n+1}}{y_{n+1}^2 + z_{n+1}^2},\ 0 \right), \text{ and } \mathbf{H}_{n+1}^{zx} = \left(\frac{-x_{n+1}}{x_{n+1}^2 + z_{n+1}^2},\ 0,\ \frac{z_{n+1}}{x_{n+1}^2 + z_{n+1}^2},\ 0 \right). \quad (29)$$

For the PPS method with a single sensor, the information matrix $\mathbf{J}_n$ given in (22) can be recursively obtained using equations from (24) to (38) except the initial condition. We can assume that $\mathbf{J}_0$ is a zero matrix -- no information at all at the beginning of the estimation.

4.2 CRLB Derivation based on the Direct 3-D Method

In the direct 3-D method, the information matrix $\mathbf{J}_n$ is expressed as a 6×6 matrix, and the lower bound is directly obtained from (22) with the extension of 2-D state vector based matrices. The state transition matrix is expressed as

$$\mathbf{F}_n = \begin{pmatrix} 1 & T_s & 0 & 0 & 0 & 0 \\ 0 & 1 & 0 & 0 & 0 & 0 \\ 0 & 0 & 1 & A_y T_s^2 / 2V_{n-1}^y + T_s & 0 & 0 \\ 0 & 0 & 0 & A_y T_s / V_{n-1}^y + 1 & 0 & 0 \\ 0 & 0 & 0 & 0 & 1 & A_z T_s^2 / 2V_{n-1}^z + T_s \\ 0 & 0 & 0 & 0 & 0 & A_z T_s / V_{n-1}^z + 1 \end{pmatrix}. \tag{30}$$

5. Analysis and Simulation

In this section, the PPS and direct 3D methods are compared in terms of their simulation results and CRLB's. As the proposed method selects the smallest measurement variance, the covariance $\mathbf{R}_n$ plays an important role for the lower bound. The minimum covariances obtained via the PPS method minimize the lower bound – the PPS method flexibly chooses planes with the smallest variances. Several scenarios are considered for performance comparison. Scenario 1 and 2 show the single sensor based plane selection according to ϕ. Scenario 3 shows the changes of the plane selection from xy- and yz-planes to xy- and zx-planes according to ϕ. In all scenarios, the sensor is measuring θ and ϕ with the interval of 0.1 second and the variances of the measurements are both 3.

5.1 Scenario 1

In this scenario, an object is moving in the range of ϕ being between 45.36^o and 76.74^o as well as in the range of θ being between 45.00^o and 49.04^o. More specifically, a single sensor is placed in the origin (0*m*, 0*m*, 0*m*), and the initial position of the object is (3*m*, 3*m*, 1*m*) with an initial velocity of (1*m/s*, 1*m/s*, 1*m/s*). The observed object is moving in CV in the x-direction, in CA in the y and z directions, with $0.1m/s^2$ and $0.5m/s^2$, respectively. Since the ϕ is measured in the range between 45.36^o and 76.74^o, the xy- and yz-planes are selected. In addition, the initial object state is given.

5.2 Scenario 2

In this scenario, an object is moving in the range of ϕ being between 25.24^o and 36.26^o as well as in the range of θ being between 45.00^o and 50.28^o. Similar to scenario 1, a single sensor is placed at the origin (0*m*, 0*m*, 0*m*) with the same initial object velocity and movement. The initial object position is (1*m*, 1*m*, 3*m*). Since ϕ is in the range between 25.24^o and 36.26^o, the xy- and zx-planes are selected. Also, the initial object state is given.

5.3 Scenario 3

In this scenario, an object moves in the range of ϕ being between 28.07^o and 48.24^o crossing 45^o. The sensor is placed at the origin (0*m*, 0*m*, 0*m*), and the initial position of the object is (2*m*, 1*m*, 2*m*) with an initial velocity of (0.3*m/s*, 0.3*m/s*, 0.3*m/s*). Similar to previous scenarios, the observed object is moving in CV in the x-direction, in CA in the y- and z-directions, with $0.1m/s^2$ and $0.5m/s^2$, respectively. Since ϕ of the first 13 time instants is measured between 48.24^o and 45.42^o, the xy- and yz-planes are selected. In the last 37 time instants, xy- and zx-planes are selected since ϕ is measured between 28.07^o and 44.96^o.

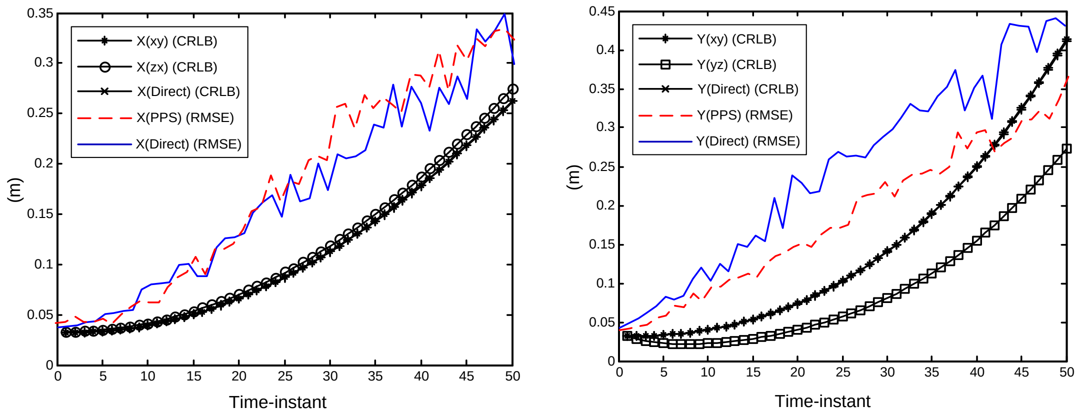

(a) CRLB X (b) CRLB Y

Fig. 7. Scenario 1: Selected xy- and yz- planes based on PPS show better performance.

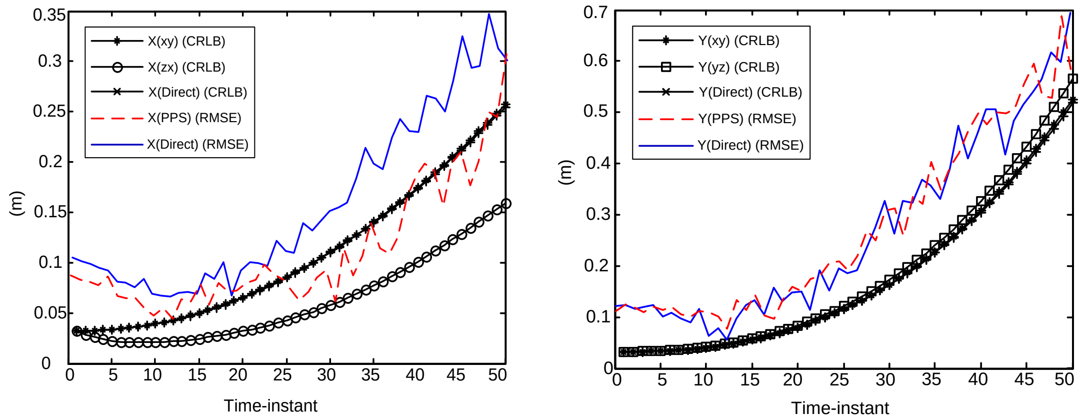

(a) CRLB X (b) CRLB Y

Fig. 8. Scenario 2: Selected xy- and zx- planes based on PPS show better performance.

5.4 Results

Fig. 7, **Fig. 8** and **Fig. 9** represent the lower bound and RMSE in each direction based on scenario 1, 2 and 3, respectively. In **Fig. 7**, selecting the yz-plane with xy-plane and in **Fig. 8**, selecting the zx-plane with xy- plane show good performance, which proves that the PPS method is a good estimator. Note that all boundaries are presented for comparing the selection of other planes. In addition, a dynamic plane selection is shown in simulated in **Fig. 9**. Also, note that PF we use is known as the best estimator in nonlinear and non-Gaussian tracking problem. Under the condition with linear and Gaussian tracking problem, Kalman filter with PPS method will provide the optimum estimation in 3-D space.

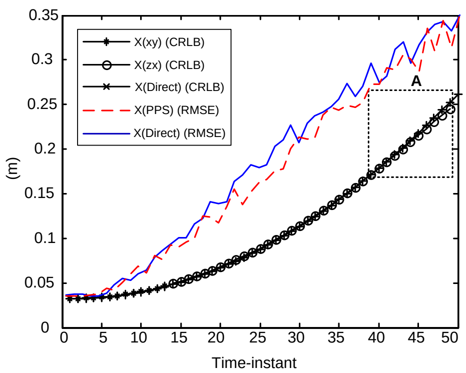

(a) CRLB X

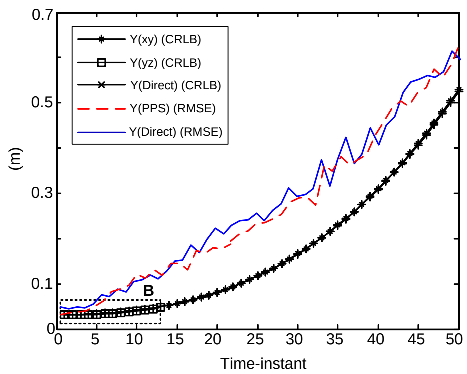

(b) CRLB Y

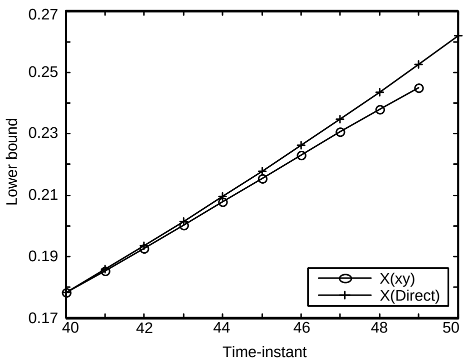

(c) Enlargement of A section

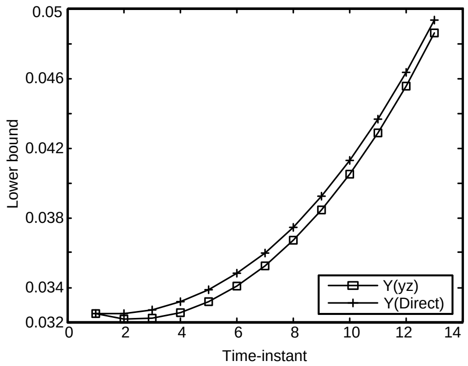

(d) Enlargement of B section

Fig. 9. Scenario 3: The first 13 time instants xy- and yz-planes are selected, and the last 37 time instants, the xy- and zx-planes are selected. For the performance comparison between PPS and direct 3D method, the certain section in CRLB is enlarged (A and B).

5.5 Computational Complexity Comparison

Fig. 10 shows the simplified overall flows of PPS and direct method, where PPS performs multiple 2-D particle filters, and direct method performs single 3-D particle filter. In the case of sphere density with radius r, direct method ideally requires πr^3 particles wile PPS method requires πr^2 particles. It means that direct method requires $r^{\frac{3}{2}}$ time particles and its corresponding computational resources. Thus, under dual processors available, PPS method has $r^{\frac{3}{2}}$ time less complexity.

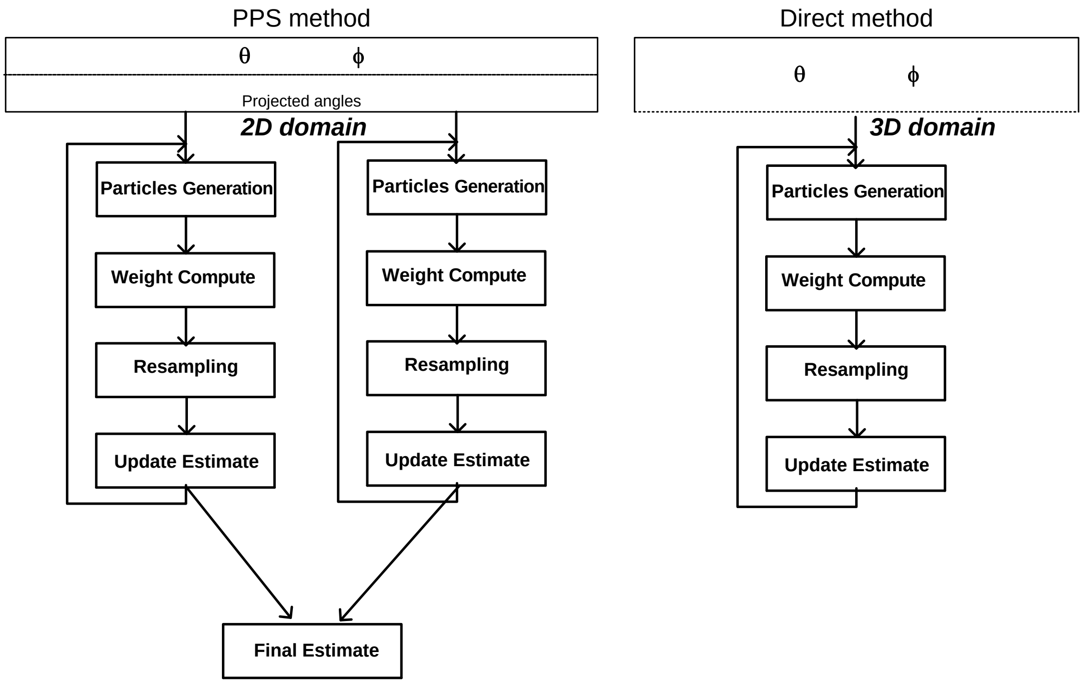

Fig. 10 Simplified algorithmic flows of PPS and direct method.

6. Conclusions

We have proposed an object tracking algorithm in 3-D space with a passive acoustic sensor. The particle filtering technique used in the 2-D bearings-only tracking problem has been applied to the 3-D space. 3-D space is decomposed into 2-D planes, and by exploiting the fact that the noisy measurements of the acoustic sensor differ on the projected planes, we have proved the effectiveness of the plane selection based on the characteristics. We have shown that the particle filtering with the proposed plane selection is more flexible than the direct 3-D method where the proposed method can be easily extended to multiple sensor particle filtering. We have also analyzed the performance of the proposed method using the Cramer-Rao Lower Bound (CRLB) and the theoretical lower bound, and the simulation results are compared to those of the direct 3-D method. We have shown that the proposed method outperforms the direct 3-D method.

References

[1] C.H. Knapp, G.C. Carter, "The Generalized Correlation Method of Estimation of Time Delay," *IEEE Trams. on Acoustics, Speech and Signal Processing*, vol. 24, no. 4, pp. 320-327, 1976. Article (CrossRef Link)

[2] J.H. Dibiase, H.F. Silverman, M.S. Brandstein, "Robust Localization in Reverberant Rooms," *Microphone Arrays: SignalProcessing Techiniques and Applications*, pp. 157-180, 2001.

[3] N. Strobel, T. Meier, R. Rabenstein, "Speaker Localization using Steered Filtered-and-sum Beamformers," in *Proc. of Erlangen Workshop on Vision, Modeling, and Visualization*, pp. 195-202, 1999.

[4] J. Vermaak, A. Blake, "Nonlinear Filtering for Speaker Tracking in Noisy and Reverberant Environments," in *Proc. of IEEE Conf. on Acoustics, Speech and Signal Processing*, pp. 3021-3024, May 2001. Article (CrossRef Link)

[5] D.B. Ward, R.C. Williamson, "Particle Filter Beamforming for Acoustic Source Localization in a Reverberant Environment," in *Proc. of IEEE Conf. on Acoustics, Speech and Signal Processing*, pp. 1777-1780, May 2002. Article (CrossRef Link)

[6] A. Doucet, N. de Freitas, N. Gordon, "Sequential Monte Carlo Methods in Practice," Springer Science and Business Media Inc., 2001.

[7] W.R. Gilks, C. Berzuini, "Following a Moving Target – Monte Carlo Inference for Dynamic Bayesian Models," *Journal of the Royal Statistical Society, B*, vol. 63, pp. 127-146, 2001. Article (CrossRef Link).

[8] P.M. Djurić, J.H. Kotecha, J. Zhang, Y. Huang, T. Ghirmai, M.F. Bugallo, J. Miguez, "Particle Filtering," *IEEE Signal Processing Magazine*, vol. 20, no. 5, pp. 19-38, 2003. Article (CrossRef Link).

[9] M.S. Arulampalam, S. Maskell, N. Gordon, T. Clapp, "A Tutorial on Particle Filters for Online Nonlinear/non-Gaussian Bayesian Tracking," *IEEE Trans. on Signal Processing*, vol. 50, no. 2, pp. 174-188, 2002. Article (CrossRef Link).

[10] D.B. Ward, E.A. Lehmann, R.C. Williamson, "Particle Filtering Algorithms for Tracking an Acoustic Source in a Reverberant Environment," *IEEE Trans. on Speech and Audio Processing*, vol. 11, no. 6, pp. 826-836, 2003. Article (CrossRef Link).

[11] J.M. Passerieux, D.V. Cappel, "Optimal Observer Maneuver for Bearings-only Tracking," *IEEE Trans. on Aerospace and Electronic Systems*, vol. 34, no. 3, pp. 777-788, 1998. Article (CrossRef Link).

[12] R.A. Iltis, K.L. Anderson, "A Consistent Estimation Criterion for Multisensor Bearings-only Tracking," *IEEE Trans. on Aerospace and Electronic Systems*, vol. 32, no. 1, pp. 108-120, 1996. Article (CrossRef Link).

[13] M.S. Arulampalam, B. Ristic, N. Gordon, T. Mansell, "Bearings-only Tracking of Manoeuvring Targets using Particle Filters," *EURASIP Journal on Applied Signal Processing*, vol. 2004, no. 1, pp. 2351-2365, 2004. Article (CrossRef Link).

[14] J. Lee, S. Hong, N. Moon, S. Oh, "Acoustic Sensor-Based Multiple Object Tracking with Visual Information Association," *EURASIP Journal on Applied Signal Processing*, vol. 2010. Article (CrossRef Link).

[15] K. Dogancay, G. Ibal, "Instrumental Variable Estimator for 3D Bearings-only Emitter Localization," in *Proc. of IEEE Conf. on Intelligent Sensors, Sensor Networks and Information Processing*, pp. 63-68, 2005. Article (CrossRef Link).

[16] H.W. Tian, Z.L. Jing, S.Q. Hu, J.X. Li, H. Leung, "Tracking a 3D Maneuvering Target using High-rate Bearings-only Measurements," in *Proc. of IEEE Int'l Conf. on Machine Learing and Cybenetics*, vol. 2, pp. 845-850, 2004. Article (CrossRef Link).

[17] M. Stanacevic, G. Cauwenberghs, "Micropower Gradient Flow Acoustic Localizer," *IEEE Trans. on Circuits and Systems I*, vol. 52, no. 10, pp. 2148-2157, 2005. Article (CrossRef Link).

[18] J. Lee, J. Lim, S. Hong, P. Park, "Tracking an Object in 3-D Space using Particle Filtering based on Sensor Array," in *Proc. of IEEE Int'l Conf. on Computer and Information Technology*, pp. 242-242, 2006. Article (CrossRef Link).

[19] B. Ristic, S. Arulampalam, N. gordon, "Beyond the Kalman filter: Particle Filter for Tracking Application," Artech House Publishers, 2004.

[20] M. Bolic, P.M. Djurić, S. Hong, "Resampling Algorithms and Architectures for Distributed Particle Filters," *IEEE Trans. on Signal Processing*, vol. 53, no. 7, pp. 2442-2450, 2005. Article (CrossRef Link).

[21] M.F. Bugallo, T. Lu, P.M. Djurić, "Target Tracking by Multiple Particle Filtering," in *Proc. of IEEE Aerospace Conf.*, pp. 1-7, 2007. Article (CrossRef Link).

[22] N. Vaswani, "Additive Change Detection in Nonlinear Systems with Unknown Change Parameters," *IEEE Trans. on Signal Processing*, vol. 55, no. 3, pp. 859-872, 2007. Article (CrossRef Link).

[23] F. Gustafsson, F. Gunnarsson, N. Bergman, U. Forssell, J. Jansson, R. Karlsson, P. Nordlund, "Particle Filters for Positioning, Navigation, and Tracking," *IEEE Trans. on Signal Processing*, vol. 50, no. 2, pp. 425-437, 2002. Article (CrossRef Link).
[24] B. Ristic, M.S. Arulampalam, "Tracking a Manoeuvring Target using Angle-only Measurements : Algorithms and Performance," *Signal Processing*, vol. 83, no. 6, pp. 1223-1238, 2003. Article (CrossRef Link).
[25] P. Tichavsky, C.H. Muravchik, A. Nehorai, "Posterior Cramer-Rao Bounds for Discrete-time Nonlinear Filtering," *IEEE Trans. on Signal Processing*, vol. 46, no. 5, pp. 1386-1396, 1998. Article (CrossRef Link).
[26] J.H. Taylor, "The Cramer-Rao Estimation Error Lower Bound Computation for Deterministic Nonlinear Systems," *IEEE Trans. on Automatic Control*, vol. 24, no. 2, pp. 343-344, 1979. Article (CrossRef Link).

Jinseok Lee received the dual B.S. degree in electrical engineering from both Stony Brook University – State University of New York and Ajou University – Korea; and the Ph.D. degree in Electrical engineering from Stony Brook University. Currently, he is a Postdoctoral Associate of Biomedical Engineering at Worcester Polytechnic Institute. His current research interests include medical instrumentation, biomedical signal processing, acoustic/image signal processing and identification, and modeling of physiological systems.

Shung Han Cho received B.E. degree (Summa Cum Laude) with specialization in Telecommunications from both the department of Electronics Engineering at Ajou University, Korea and the department of Electrical and Computer Engineering at Stony Brook University - SUNY, NY in 2006. He was a recipient of Award for Academic Excellence in Electrical Engineering by College of Engineering and Applied Sciences at Stony Brook University. He received M.S. degree with Award of Honor in Recognition of Outstanding Achievement and Dedication and Ph.D. degree in Electrical and Computer Engineering from Stony Brook University in 2008 and 2010 respectively. He is currently a post-doctoral researcher at Stony Brook University. He was a recipient for International Academic Exchange Program supported by Korea Research Foundation (KRF) in 2005. He was a member of Sensor Consortium for Security and Medical Sensor Systems sponsored by NSF Partnerships for Innovation from 2005 to 2006. His research interests include collaborative heterogeneous signal processing, distributed digital image processing and communication, networked robot navigation and communication, heterogeneous system modeling.

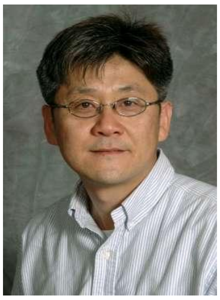

Sangjin Hong received the B.S and M.S degrees in EECS from the University of California, Berkeley. He received his Ph.D in EECS from the University of Michigan, Ann Arbor. He is currently with the department of Electrical and Computer Engineering at Stony Brook University. Before joining Stony Brook University, he has worked at Ford Aerospace Corp. Computer Systems Division as a systems engineer. He also worked at Samsung Electronics in Korea as a technical consultant. His current research interests are in the areas of multimedia wireless communications and digital signal processing systems, reconfigurable VLSI Systems and optimization. Prof. Hong is a Senior Member of IEEE and a member of EURASIP journal editorial board. Prof. Hong served on numerous Technical Program Committees for IEEE conferences.

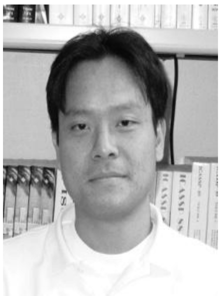

Jaechan Lim received the B.S. degree in Physics from Korea University, Seoul, Korea in 1996, and the M.S. and Ph.D. degrees in Electrical Engineering from Stony Brook University (SUNY), Stony Brook, New York in 1999 and 2007, respectively. His research areas include statistical signal processing and control, Bayesian estimation, particle filtering, channel estimation, channel equalization, and operations of wireless access network and communication systems. He was an Adjunct Professor in the Department of Electrical Engineering in the University of Bridgeport, Bridgeport, CT US. Currently, he is with the Department of Electronic Engineering in Sogang University, Seoul, Korea as a Research Professor.

Seong-Jun Oh received the B.S. (magna cum laude) and M.S. degrees in electrical engineering from Korea Advanced Institute of Science and Technology (KAIST) in 1991 and 1995, respectively, and received Ph.D. at the Department of Electrical Engineering and Computer Science, The University of Michigan, Ann Arbor in September 2000. He served for Korean Army during 1993-1994. He is currently an associate professor at the department of Computer and Communications Engineering, Korea University, Seoul, Korea. Before joining Korea University in September 2007, he was with Ericsson Wireless Communication, San Diego, California, USA as a senior engineer from September 2000 to March 2003 and with Qualcomm CDMA Technologies (QCT), San Diego, California, USA as a staff engineer from September 2003 to August 2007. His current research interests are in the area of wireless/mobile networks with emphasis on the next-generation (4G) cellular networks, resource allocation, and physical-layer modem implementation.